

# Analysis of Multidomain Protein Dynamics

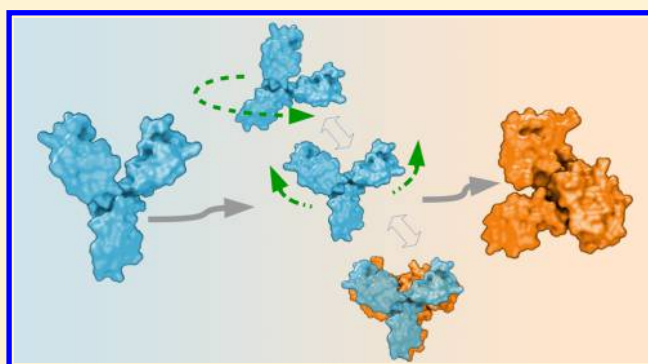
Amitava Roy,<sup>\*,†</sup> Duy P. Hua,<sup>‡,¶</sup> and Carol Beth Post<sup>‡,¶</sup>

<sup>†</sup>Bioinformatics and Computational Biosciences Branch, Rocky Mountain Laboratories, NIAID, National Institutes of Health, Hamilton, Montana 59840, United States

<sup>‡</sup>Medicinal Chemistry and Molecular Pharmacology and <sup>¶</sup>Markey Center for Structural Biology, Purdue University, West Lafayette, Indiana 47907, United States

**S** Supporting Information

**ABSTRACT:** Proteins with a modular architecture of multiple domains connected by linkers often exhibit diversity in the relative positions of domains, while the domain tertiary structure remains unchanged. The biological function of these modular proteins, or the regulation of their activity, depends on the variation in domain orientation and separation. Accordingly, careful characterization of interdomain motion and correlated fluctuations of multidomain systems is relevant for understanding the functional behavior of modular proteins. Molecular dynamics (MD) simulations provides a powerful approach to study these motions in atomic detail. Nevertheless, the common procedure for analyzing fluctuations from MD simulations after rigid-body alignment fails for multidomain proteins; it greatly overestimates correlated positional fluctuations in the presence of relative domain motion. We show here that expressing the atomic motions of a multidomain protein as a combination of displacement within the domain reference frame and motion of the relative domains correctly separates the internal motions to allow a useful description of correlated fluctuations. We illustrate the methodology of separating the domain fluctuations and local fluctuations by application to the tandem SH2 domains of human Syk protein kinase and by characterizing an effect of phosphorylation on the dynamics. Correlated motions are assessed from a distance covariance rather than the more common vector-coordinate covariance. The approach makes it possible to calculate the proper correlations in fluctuations internal to a domain as well as between domains.



## 1. INTRODUCTION

Changes in domain structure are fundamental to the biological function of certain proteins with a modular architecture of multiple domains connected by linkers. The essence of molecular machines, signaling proteins, and some allosteric proteins lies in the motions that alter the relative orientation between domains.<sup>1–5</sup> Further, for enzymes in which the active site is formed from multiple domains, concerted domain motions can greatly influence the positioning of catalytic residues and thus regulate catalytic activity.<sup>3</sup> In another example, the modular structure of a protein can serve to form a binding surface across domains so that variation in domain structure is the basis for regulating the interaction with binding partners.<sup>1,6</sup>

Characterizing the dynamics of multidomain proteins in terms of positional fluctuations and correlated motions using molecular dynamics (MD) simulation is a powerful and often-practiced first step toward elucidating molecular behavior and function, mechanisms of regulation of modular proteins, and allostery. For the case of allosteric function of modular proteins in particular, discovering correlations in atomic fluctuations and domain motions detected over a long distance would be a key component in a description of the molecular mechanism of allostery. While changes in motional time scales over a set of

amino acids due to a conformational perturbation of the protein can be determined from NMR relaxation studies,<sup>7</sup> these experiments cannot determine correlations in motions. MD studies can directly assess possible correlation networks that might form the basis of allostery.<sup>4,8,9</sup> Nevertheless, even though fluctuations and correlated motions in single domain proteins are readily analyzed, assessment of motions in a multidomain protein is complicated due to the presence of both local motions internal to the framework of an individual domain and changes in domain–domain separation and relative domain orientation, so that estimating fluctuations following the same analysis fails. One tactic that can be taken toward understanding dynamics of multidomain proteins is to account for the collective motion of a modular protein using a description of changes in the relative domain orientation plus changes in the atomic positions internal to a given domain. Such an approach is motivated by the rationale that concerted motions derived from local fluctuations translate into larger-scale domain–domain motion. To implement such an approach, and to properly assess the dynamics of multidomain proteins in general, it is essential to identify fluctuations in local structure

Received: August 18, 2015

Published: December 2, 2015

and domain structure independently to effectively characterize the dynamics of multidomain protein.

A difficulty in general with evaluating conformational flexibility of a protein from a MD trajectory is separating overall rigid-body motion from fluctuations in the internal structure<sup>10–13</sup> because there is no unambiguous way to remove the external degrees of freedom from internal dynamics of a flexible protein.<sup>11,12</sup> Separating rigid body motions from local fluctuations in the time evolution of atomic positions of a protein is an underdetermined problem (discussed in more detail in the Supporting Information (SI)), so that the result for the local fluctuation amplitudes depends on the assumptions made to define the rigid-body molecule frame. The most popular assumption is to remove the overall motion by a single rigid body alignment that minimizes the difference in coordinates of all atoms, or a relatively rigid subset of atoms, between the flexible protein conformation (a trajectory snapshot) and a reference structure.<sup>10,11,14</sup> While this common approach is reasonable for a single domain protein where the choice for a structural core is readily apparent, further thought is needed to characterize internal motions of a modular multidomain protein. In the case that relative domain orientation varies in a multidomain protein, a single alignment step to minimize the difference between the reference structure and a trajectory snapshot does not separate motions within a domain from motions between domains.

We introduce here a procedure with two alignment steps that gives accurate fluctuation values and therefore reasonable estimates for a correlation analysis of internal motions and rigid-body domain motions as validated with a known system (see the SI). We demonstrate its application to the tandem SH2 protein, a multidomain protein fragment from the human spleen tyrosine kinase, Syk. Correlated motion is assessed using a metric based on changes in atomic positions rather than absolute atomic positions. In what follows, we first describe the overestimate of correlated motion that arises with a typical single alignment procedure for analyzing the fluctuations and covariance of the tandem SH2 protein. Next, we present a procedure that more accurately describes the fluctuations of multidomain proteins by including two rigid-body alignment steps and the resulting correlation coefficients. Finally, we apply the approach to characterize the effect of tyrosine phosphorylation on correlated internal motions and relative domain motions and, thus, illustrate how correlation analysis of multidomain proteins can give insight into their biological function.

## 2. METHODS

**2.1. Molecular Dynamics Simulations.** *Simulations of the Unphosphorylated and Phosphorylated Forms of the Syk Tandem SH2 Protein.* Two 0.5  $\mu$ s trajectories of the 254-residue, multidomain Syk tandem SH2 fragment in the unphosphorylated tSH2 and Tyr131-phosphorylated ptSH2 forms were calculated with the NAMD program using the CHARMM22/CMAP force field. The initial coordinates for tSH2 and ptSH2 simulations were taken from chain A of the asymmetric unit of the crystal structure (PDB ID: 1A81). The two proteins tSH2 and ptSH2 were solvated in octahedral boxes with 15043 TIP3P water molecules as well as Na<sup>+</sup> and Cl<sup>-</sup> ions so that the distance from the protein edge to the box edge was at least 12 Å and the salt concentration was maintained at 0.15 M. The nonbonded list was generated with a 14 Å cutoff. A switching function was applied to the van der

Waals potential energy from 10 to 12 Å to calculate nonbonded interactions. The Particle Mesh Ewald (PME) algorithm was used to calculate electrostatic interactions.

The energy of the solvated proteins was minimized first with the positions of the protein atoms fixed, then with harmonic restraints on protein backbone heavy atoms (N, C, C<sub>α</sub> atoms), and last without restraints using the steepest descent and Powell algorithms.

All trajectories were calculated using the leapfrog integrator with a 2 fs time step. The SHAKE constraint was applied to fix the lengths of bonds involving hydrogen atoms. The systems were heated from 100 to 298 K and equilibrated at 298 K in the NVE ensemble for a total of 500 ps. The appropriate system volumes of the two species were established with a 1 ns equilibration in the NPT ensemble using constant pressure and temperature (CPT) dynamics. The Nose-Hoover thermostat and Langevin barostat were used to maintain a reference temperature of 298 K and a reference pressure of 1 atm. The NPT-equilibrated systems with the proper volumes were equilibrated for 2 ns in the NVT ensemble at 298 K using a Langevin heat bath with a friction coefficient of 1 ps<sup>-1</sup>. Production runs were carried out for 0.5  $\mu$ s with coordinates saved every 1 ps, yielding one trajectory of 0.5  $\mu$ s for each form of the tandem SH2 fragment.

*Simulations of the Isolated SH2 Domain.* An isolated 96-residue SH2 domain was simulated using the NAMD program with the CHARMM22/CMAP force field. The initial coordinates of the isolated SH2 domain were taken from chain A, residues 167–262, of the asymmetric unit of the crystal structure (PDB ID: 1A81). The isolated SH2 domain was solvated in an octahedral box filled with 7817 TIP3P water molecules and Na<sup>+</sup> and Cl<sup>-</sup> ions so that the distance between the protein and box edges was at least 12 Å and the salt concentration was 0.15 M.

A 0.1  $\mu$ s trajectory of the isolated SH2 domain was calculated using the same simulation conditions as those used to calculate the trajectories of the unphosphorylated and phosphorylated tandem SH2 fragments.

**2.2. Separation of Motions.** We provide a mathematical description for the separation of motions and first present the common approach of modeling atomic displacements as a combination of rigid-body motion and deviations from it. Let us assume  $\mathbf{R}_t$  represents position vectors of  $N$  atoms in the  $t$ th snapshot of a MD trajectory, with  $\mathbf{R}_t^i$  being the position vector of the  $i$ th atom, at time  $t$ .

Then without any loss of generality we can write for time  $t$

$$\begin{aligned}\mathbf{R}_t &= \mathbf{T}_t + \mathbf{U}_t \mathbf{R}_0 + \boldsymbol{\delta}_t \\ \mathbf{U}_t^{-1} \boldsymbol{\delta}_t &= \mathbf{U}_t^{-1} (\mathbf{R}_t - \mathbf{T}_t) - \mathbf{R}_0\end{aligned}\quad (1)$$

where  $\mathbf{T}_t$  is the overall translation vector,  $\mathbf{R}_0$  is the position of the  $N$  atoms in the reference structure,  $\mathbf{U}_t$  is the matrix representing overall rotation of the protein molecule with respect to the reference structure, and  $\boldsymbol{\delta}_t$  is the deviation of the  $i$ th atom from the rigid-body motion of  $\mathbf{T}_t$  and  $\mathbf{U}_t$ .  $\mathbf{U}_t^{-1}$  is the inverse matrix of  $\mathbf{U}_t$ . Overall translation is removed by aligning the center of mass (COM) of the conformation at time  $t$  with that of the reference structure. Typically for a single domain protein,  $\mathbf{U}_t^{-1}$  is found by aligning the flexible structure to the reference structure to minimize  $\sum_{i \in \{M\}} \|\mathbf{R}_t^i - \mathbf{U}_t \mathbf{R}_0^i - \mathbf{T}_t\|^2$ , where  $\{M\}$  is a subset of atoms spanning the whole protein.<sup>10,11,14</sup> The time series  $\boldsymbol{\delta}_t$  represents the deviation of the atoms from the rigid body motion. Once  $\mathbf{U}_t$  and subsequently  $\mathbf{U}_t^{-1} \boldsymbol{\delta}_t$  are

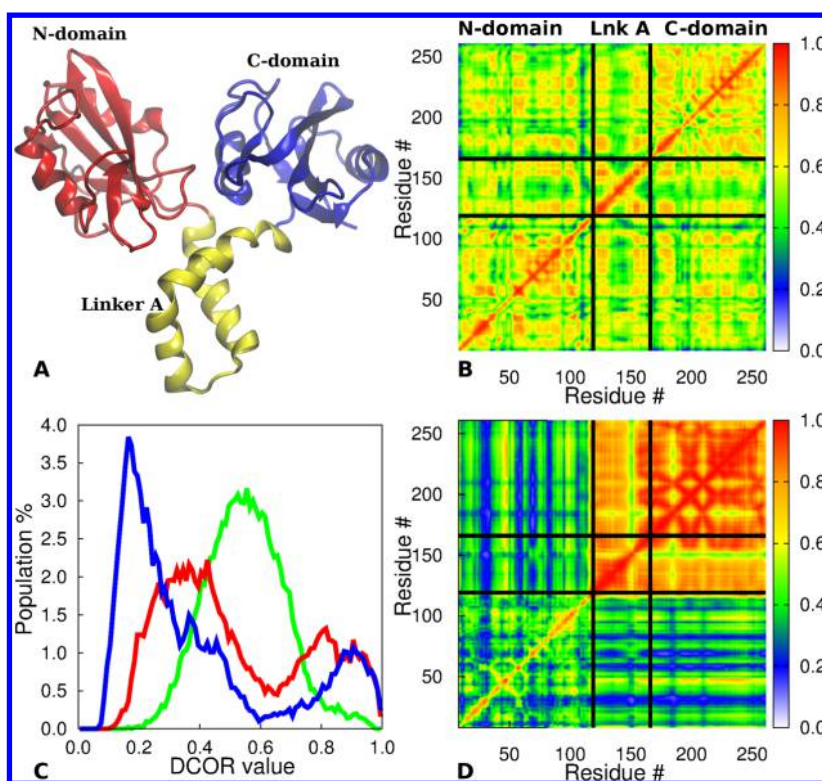


**Figure 1.** Covariance analysis of  $C_{\alpha}$ - $C_{\alpha}$  positions of tSH2 protein using a single overall alignment and the distance correlation coefficients,  $DCOR$ , calculated from a  $0.5 \mu\text{s}$  trajectory. (A) Ribbon representation of Syk tSH2 protein (PDB ID 1A81) with the SH2<sub>N</sub> (residues 9–119) in red, linker A (residues 120–166) in gold, and SH2<sub>C</sub> (residues 167–262) in blue. Residue numbering is for the human Syk protein. (B)  $DCOR$  values between  $C_{\alpha}$  atoms calculated after whole-molecule least-squares alignment with respect to all  $C_{\alpha}$  atoms. The presence of domain fluctuations gives rise to the apparent high  $DCOR$  values. (C) Histograms of  $DCOR$  values after a single alignment with respect to either  $C_{\alpha}$  atoms of all residues (green) or residues in the SH2<sub>N</sub> (red) or SH2<sub>C</sub> (blue). The green curve corresponds to the cross correlation values in B. That the histogram profile changes drastically depending on how the structures are aligned is unsatisfactory and indicates the presence of domain fluctuation. (D)  $DCOR$  values after alignment with respect to the SH2<sub>N</sub> plotted in the red histogram in C.

estimated, cross correlation or other properties, such as root-mean-square fluctuation (RMSF), can be calculated from  $\delta_t$ .

In the case of multidomain protein, changes in the relative orientation of domains also contribute to the total atomic displacements; the overall motion, relative domain fluctuations (DF), and local fluctuations within a domain (LF) can be separated following a procedure in the spirit of eq 1. Let us consider a protein with  $D$  domains. We can write the position of the  $i$ th atom at time  $t$  as a combination of overall motion, LF and DF with the constraint that DF does not give rise to overall rotation or translation:

$$\mathbf{R}_t = \mathbf{T}_t + \mathbf{U}_t[\mathbf{S}_t^1 + \mathbf{W}_t^1\mathbf{R}_0^1 \dots \mathbf{S}_t^D + \mathbf{W}_t^D\mathbf{R}_0^D] + \delta_t \quad (2)$$

In the above equations  $\mathbf{S}_t^d$  and  $\mathbf{W}_t^d$  represent the independent translation and rotation of the  $d$ th domain within the overall molecular frame at time  $t$ , respectively.  $\mathbf{R}_0^d$  in the above equation represents the position vector of the atoms in the  $d$ th domain of the reference structure. Any rotation matrix, other than the identity matrix, leaves only the center point unchanged. Since the  $\mathbf{W}_t^d$  matrices leave the centers of the domains unchanged, the domain rotations in eq 2 cannot contribute to overall rotation. Furthermore,  $\mathbf{S}_t^d$  matrices in eq 2 represent relative translations of the domains and do not contribute to overall translation. We can rewrite eq 2 as

$$\mathbf{U}_t^{-1}\delta_t^i = \mathbf{U}_t^{-1}(\mathbf{R}_t - \mathbf{T}_t) - \mathbf{R}_t' \quad (3)$$

where  $\mathbf{R}_t' = [\mathbf{S}_t^1 + \mathbf{W}_t^1\mathbf{R}_0^1 \dots \mathbf{S}_t^D + \mathbf{W}_t^D\mathbf{R}_0^D]$

To separate LF and DF according to eq 3 the following protocol is applied to each snapshot of the original trajectory to generate two trajectories, as schematically illustrated in Figure 2.

1. Remove the molecule translation and rotation by least-squares superposition of the snapshot with respect to the reference structure using atoms selected over the whole protein (step 1 in Figure 2 and  $\mathbf{U}_t^{-1}(\mathbf{R}^t - \mathbf{T}^t)$  in eq 3).

2. Obtain the rigid-domain trajectory by independently aligning individual domains of the reference structure to the corresponding domain of the oriented snapshot (step 2 in Figure 2 and  $\mathbf{R}_t'$  in eq 3) and keeping coordinates of the aligned reference domains.

3. Obtain the LF trajectory from the coordinate difference between the oriented reference domains and the oriented snapshot domain (step 3 in Figure 2 and  $\mathbf{U}_t^{-1}\delta_t^i$  in eq 3). The rigid-domain trajectory generated in step 2 is used to estimate domain–domain correlation, while the LF trajectory obtained in step 3 is used to calculate correlations in the local atomic fluctuations.

**2.3. Distance Correlation.** In this work, we calculated correlation using a distance correlation coefficient,  $DCOR$ .<sup>15</sup> Previously, we showed that among Pearson's correlation coefficient (PCC), a generalized correlation coefficient (GCC)<sup>16</sup> and  $DCOR$ ,  $DCOR$  is the most appropriate parameter to find association in atomic motions because it is least sensitive to angular dependence while reflecting variability in covariance.<sup>17</sup>

Calculation of *DCOR* between two vector series is straightforward to implement. Let  $\{\mathbf{A}\}$  and  $\{\mathbf{B}\}$  be two vector series with  $m$  entries each and the  $i$ th entry in  $\{\mathbf{A}\}$  is denoted by  $\mathbf{A}^i$ . To calculate distance covariance between  $\{\mathbf{A}\}$  and  $\{\mathbf{B}\}$  the following five steps are needed.

1. Calculate the  $m \times m$  matrix,  $\mathbf{a}$ , from  $\{\mathbf{A}\}$ , where  $a_{ij}$  is the Euclidean distance between the  $i$ th and  $j$ th entries of  $\{\mathbf{A}\}$ :  $a_{ij} = |\mathbf{A}^i - \mathbf{A}^j|$
2. Average the rows of  $\mathbf{a}$ :  $a_i = \frac{1}{m} \sum_j a_{ij}$
3. Average the columns of  $\mathbf{a}$ :  $a_j = \frac{1}{m} \sum_i a_{ij}$
4. Average all elements of  $\mathbf{a}$ :  $a_{..} = \frac{1}{m^2} \sum_{ij} a_{ij}$
5. Build the  $m \times m$  matrix  $\alpha$  from  $\mathbf{a}$  where  $\alpha_{ij} = a_{ij} - a_i - a_j + a_{..}$ .

Then the distance covariance is

$$\text{cov}(\mathbf{A}, \mathbf{B}) \equiv \sqrt{\frac{1}{m^2} \sum_{ij} \alpha_{ij} \beta_{ij}} \quad (4)$$

where  $\beta_{ij}$  is defined similarly from  $\mathbf{B}$ .

The distance correlation coefficient, *DCOR*, is defined as

$$\text{DCOR} \equiv \frac{\text{cov}(\mathbf{A}, \mathbf{B})}{\sqrt{\text{cov}(\mathbf{A}, \mathbf{A})\text{cov}(\mathbf{B}, \mathbf{B})}} \quad (5)$$

*DCOR* was found to capture both linear and nonlinear correlation between positional vectors.<sup>17</sup> In an earlier study we observed long-distance concerted motions in a protein using *DCOR* that was not revealed by PCC or GCC.<sup>17</sup>

### 3. RESULTS AND DISCUSSION

**3.1. Single Alignment Overestimates Domain Fluctuation in Tandem SH2.** The effect of relative domain fluctuations on estimates correlation coefficients using the common procedure of a single rigid-body alignment step is illustrated for the Syk tandem SH2 (tSH2), a multidomain protein comprising two SH2 domains, SH2<sub>N</sub> and SH2<sub>C</sub> connected by a flexible linker A (see Figure 1A). The cross correlations in dynamics between 254  $C_\alpha$  atoms were calculated from a 0.5  $\mu\text{s}$  trajectory of the tSH2 (see the Methods section). We used a distance correlation coefficient, *DCOR*,<sup>15</sup> rather than the more common vector coordinate, Pearson's correlation coefficient (PCC), to evaluate the correlated motion. *DCOR* measures the correlation in the change in atomic positions over a time period, that is the correlation in Euclidean distance of the atomic position at time  $t$  and  $t + \delta t$ . *DCOR* is the most powerful parameter among conventional metrics for assessing correlated fluctuation in protein motion because it can capture the true correlation, both linear and nonlinear, between positional vectors.<sup>17,18</sup> The mathematical definition of *DCOR* is provided in the Methods section.

To characterize covariation in internal motions of the tSH2 protein, we first consider positional correlations calculated following a single overall alignment. Conformations obtained from 0.5  $\mu\text{s}$  trajectory were aligned following the common procedure of least-squares superposition to minimize the difference in all  $C_\alpha$  coordinates of each snapshot with the coordinates of a reference structure, the initial structure in this case. *DCOR* values after a single alignment of the whole molecule are shown in Figure 1B, and the histogram of these *DCOR* values is shown in Figure 1C (green curve). All correlation coefficients are unreasonably high for covariance of fluctuations within a domain with a mean value around 0.6,

compared to 0.3 calculated from a MD trajectory of a single SH2 domain in a previous study.<sup>17</sup> The unusually high correlation arises from the presence of domain–domain motions that are not separated from the motion internal to a domain by a single overall alignment of the flexible target with the reference structure.

Another approach that has been taken in previous studies is to align the trajectory ensemble with respect to a single domain and then examine correlations between atoms in two domains.<sup>19</sup> This approach shows that correlation values for atoms within the chosen domain agree with expected values; however, this approach greatly overestimates the correlation between and within the remaining domains. This behavior is demonstrated here by a single alignment of the tSH2 conformational ensemble with the SH2<sub>N</sub> domain (residues 9–119) (Figure 1D). Although the cross correlations between  $C_\alpha$  atoms within SH2<sub>N</sub> or between SH2<sub>N</sub> and other domains are small and most are less than 0.6, correlations between atom pairs that are either intradomain or interdomain pairs from the other two domains, linker A (residues 120–166) and SH2<sub>C</sub> (residues 162–262), are generally greater than 0.8, again indicating much stronger covariance in motions overall than anticipated for proteins. A histogram of these *DCOR* values (Figure 1C, red) further illustrates the strong sensitivity to the selection of atoms for a single-alignment procedure. In comparison to the histogram of *DCOR* values calculated after a single alignment of all  $C_\alpha$  atoms (Figure 1C, green curve), the distributions calculated by aligning to  $C_\alpha$  atoms of either the SH2<sub>N</sub> (Figure 1C, red curve) or the SH2<sub>C</sub> (blue curve) domain are highly populated at a smaller *DCOR* value, yet the population with *DCOR* value greater than 0.8 increases substantially. The variability in *DCOR* distributions shown in Figure 1C is clearly unsatisfactory for characterizing any kind of relative domain–domain motion; correlations between domains cannot be characterized reliably with any choice of atoms using a single alignment.

**3.2. Approach To Separate Local and Domain Fluctuation.** We propose a simple procedure that better describes positional fluctuations in the internal structure of modular proteins by separating the relative domain fluctuations, DF, and the local fluctuations within a domain, LF, under the assumption that these internal motions and the overall rigid-body motion are independent. Details of the mathematical formulation for our protocol are given in the Methods section. The procedure involves two alignment steps, shown schematically in Figure 2. The whole protein structure taken from trajectory snapshots is superposed with the reference structure to remove overall translation and rotation (step 1, first alignment). Each domain of the reference structure is then aligned to the corresponding domain of the superposed snapshot structures to obtain the relative domain fluctuation (step 2, second alignment). The difference in coordinates generated from the two alignment steps is the local fluctuations (LF) within a domain (step 3). The accuracy in the description of the total atomic motion using this approach is demonstrated by application to a model trajectory in which the local fluctuation amplitudes and fluctuations in relative domain positions are known (discussed in the SI).

We recognize that there are situations in which the assumption that protein internal motions are independent of overall rotation is invalid. For example, changes in the shape of a flexible body with zero angular momentum can induce changes in external orientation.<sup>20</sup> Consequently, rotation

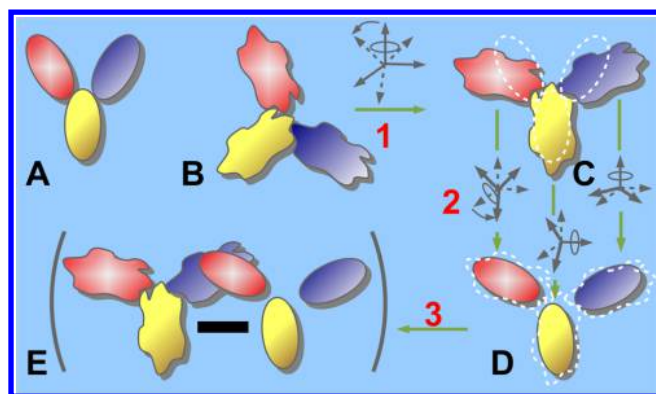


**Figure 2.** Schematic to illustrate the separation of LF and DF in a flexible multidomain protein. (A) and (B) show the reference and the flexible structure (trajectory snapshot), respectively. (C) In step (1) the flexible structure is aligned with the reference structure to remove the overall motion and generate the oriented structure. (D) In step (2) individual domains of the reference structure are aligned with (C) to specify the domain fluctuation, DF. (E) In step (3), the coordinate difference between the oriented structure C and the structure D with rigid domain motion gives the local fluctuation, LF.

cannot be completely separated from internal motion of a flexible object without *a priori* knowledge of the deformability of the object during rotation.<sup>20</sup> Zhou et al. demonstrated that, in simulating a microcanonical ensemble, a protein molecule undergoes larger rigid body motion than allowed from the conservation of angular momentum as a consequence of the flexibility of the protein molecule.<sup>13</sup> The dependency of the internal fluctuation and the overall rigid-body motion has also been pointed out in calculation of NMR variables related to global and local motions.<sup>21</sup> These cases indicate that overall rigid-body motion and internal fluctuations are not entirely independent. Nevertheless, the coupling is difficult to quantify but certainly weaker for less deformable bodies. We note that this independence is implicitly assumed in general for the removal of overall rotation from single-domain proteins. Here, we extend the same assumption to multidomain proteins even though the assumption is not strictly valid. We do so in order to provide a more robust protocol for describing correlated motions between all regions of the protein than using the current single-alignment approach.

Following our approach to decompose the total atomic displacements, the final step 3 captures the displacements due to motions internal to a domain framework. Accordingly, the rms fluctuations calculated from this difference LF trajectory in the case of tSH2 should be similar to fluctuations determined from a trajectory of an isolated SH2 domain if there are no effects on motions due to the presence of the other domains. We therefore compare the values of the rms fluctuations calculated from the LF trajectory of tSH2 with the values calculated from a trajectory of an isolated domain. The results for the main chain rms fluctuations are plotted in Figure 3 as a function of residue number for the isolated C-terminal SH2 domain (red) and from the LF trajectory of tSH2 (black). Examination of Figure 3 finds that the fluctuation profiles are indeed highly similar to the same pattern of larger fluctuations for the loops and smaller values near 0.5 Å corresponding to the helical and strand regions. The low fluctuation amplitude for the residues 172–177 seen with the tandem SH2 is a result of interactions with the linker region. The absence of the linker region in the simulation of the isolated SH2 domain, therefore,

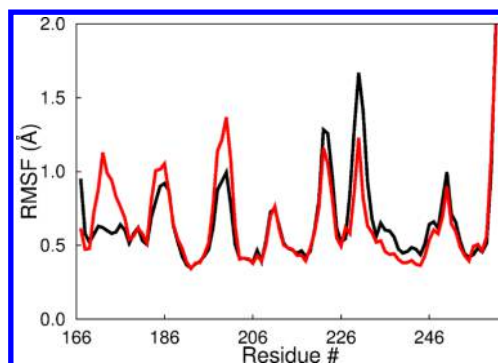


**Figure 3.** Comparison of positional fluctuations calculated from the LF trajectory of tSH2 with fluctuations calculated from an isolated SH2 domain trajectory. Residue averages of the backbone heavy atoms (N, C, and C $\alpha$  atoms) positional fluctuations calculated from the LF trajectory of the tandem SH2 (black) show similar profiles as those from the trajectory of an isolated SH2 domain (red). The large difference in fluctuation amplitude for the residues 172–177 is a result of interactions with the linker region of the tandem SH2, which is not present in the simulation of the isolated SH2 domain.

resulted in a large difference in fluctuation amplitude for the residues 172–177. Overall, the close agreement between the rms fluctuations calculated from the LF trajectory of tSH2 and the trajectory of the same SH2 domain in isolation validates the approach to separate local and domain motions.

To demonstrate the effectiveness of separating relative domain motion in a protein from local fluctuations using two rigid-body alignment steps, we compare the values for a C $\alpha$ -C $\alpha$  covariance analysis of tSH2 after separation of domain fluctuations and local fluctuations (Figure 4A) obtained with the results using a single alignment shown in Figure 1. The DCOR values for local fluctuations determined from the LF trajectory (step 3, Figure 2) are overall smaller. In particular the interdomain DCOR values are found to be in the range 0.2 to 0.3 compared to 0.5 to 0.7 without separation of motions (Figure 1B). The average difference between the interdomain cross correlation values of Figure 1B and Figure 4A is  $0.38 \pm 0.31$ . The distribution of LF DCOR values of tSH2 after removing DF is in Figure 4B (green). Most correlation values are <0.4, and the DCOR distribution is unlike any of the distributions in Figure 1C. Subsets of the histogram shown by the green line are for DCOR values within the SH2<sub>N</sub> (red) and SH2<sub>C</sub> (blue). All three histograms have been normalized independently and show similar patterns of peaks near 0.3 and long tails after 0.6 corresponding to a small set of C $\alpha$ -C $\alpha$  pairs with highly correlated motions. Together, these characteristics of the DCOR distributions are as expected for proteins.

**3.3. Effect of Phosphorylation on tSH2 Dynamics.** We demonstrate that differences in domain–domain motions can be assessed using the two-alignment procedure (eq 2, Figure 2) to evaluate the effect of phosphorylation on tSH2 dynamics. The SH2<sub>N</sub>, SH2<sub>C</sub> and linker A are tightly associated in tSH2, but NMR measurements show that, upon phosphorylation of the residue Tyr-131 of linker A, the relative SH2–SH2 domain orientation changes and their rotational tumbling time diminishes, indicating the interactions between the SH2<sub>N</sub> and SH2<sub>C</sub> domains are weakened and the domains become partially decoupled,<sup>1</sup> which results in decreased affinity for the receptor in immune signaling. The resonances for linker A are too broad to be detected, and the physical basis for this effect of phosphorylation on tSH2 conformation and dynamics is

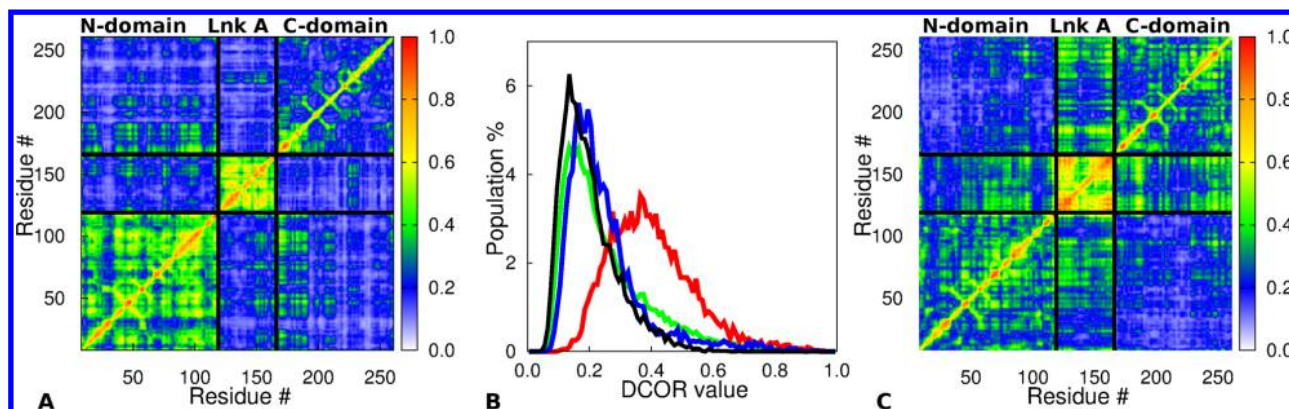


**Figure 4.** Covariance analysis of  $C_{\alpha}$ - $C_{\alpha}$  positions of tSH2 with separation of local and domain fluctuations using two alignment steps (Figure 2) and calculated from the same trajectory used for calculations shown in Figure 1. (A) DCOR values of  $C_{\alpha}$  atoms from the LF trajectory of tSH2. These values show cross correlation of local fluctuations between two atoms within a domain as well as atoms in two different domains. (B) Histograms of DCOR values from the LF trajectory of tSH2 for all  $C_{\alpha}$  atoms (green), for  $C_{\alpha}$  atoms within SH2<sub>N</sub> (red), within SH2<sub>C</sub> (blue) and  $C_{\alpha}$  atoms between domains (black). Red, blue, and black histograms are a subset of the green histogram. Each of them has been independently normalized. The profiles are very similar as might be expected. (C) DCOR values of  $C_{\alpha}$  atoms from the LF trajectory of ptSH2. The effect of phosphorylation on local fluctuations is shown by comparison with panel A. Values show cross correlation of local fluctuations between two atoms within a domain as well as in two different domains.

unknown. How phosphorylation of a residue in the linker region might cause these changes in SH2-SH2 coupling can be investigated using MD simulations following the reasoning that differences in domain coupling would be manifest in the dynamics on the time scale of MD trajectories. The two-alignment approach separating rigid-body domain motions from local motions internal to a domain would enable a reliable comparison of correlations in local motions and interdomain motions of unphosphorylated tSH2 with phosphorylated tSH2 (ptSH2). We therefore compare correlated motions from 0.5  $\mu$ s trajectories of tSH2 and ptSH2 to demonstrate the value of the approach for assessing MD trajectories, although it should be recognized that longer sampling times are needed before drawing conclusions in quantitative terms about the effects of phosphorylation.

The domain motions were characterized from the displacements of the center of mass (COM) of the three domains calculated from the DF trajectories. The covariance of the COM was computed with DCOR as a means to estimate the degree of association between two domains. Separation of the rigid body motions using the two-alignment approach allowed us to compare the association between domains and the change in association due to phosphorylation at Tyr-131 (Table 1). The correlation between the linker A and the SH2<sub>C</sub> domain is increased significantly ( $DCOR = 0.60 \pm 0.12$  to  $DCOR = 0.78 \pm 0.06$ ), indicating that a localized modification to the protein - phosphorylation at Tyr-131 - can effectively alter the global domain-domain interactions.

**Table 1.** DCOR between SH2<sub>N</sub>, SH2<sub>C</sub>, and Linker A<sup>a</sup>

	SH2 <sub>N</sub> -SH2 <sub>C</sub>	SH2 <sub>N</sub> -linker	SH2 <sub>C</sub> -linker
tSH2	$0.74 \pm 0.17$	$0.79 \pm 0.08$	$0.60 \pm 0.12$
ptSH2	$0.88 \pm 0.05$	$0.85 \pm 0.05$	$0.78 \pm 0.06$

<sup>a</sup>Distance correlation between centers of mass of SH2<sub>N</sub>, SH2<sub>C</sub>, and linker A calculated from the domain-domain motion after removal of local fluctuations. Coupling between linker A and SH2<sub>C</sub> increases upon phosphorylation of Tyr-131. The error is calculated using the moving-block bootstrap method,<sup>22</sup> which is explained in detail in the SI.

The effect of Tyr-131 phosphorylation on the intradomain motion of tSH2 can also be examined from the local fluctuation patterns of residues. DCOR values calculated from LF (Figure 3C) indicate that correlations in  $C_{\alpha}$  displacements from local fluctuations of residues within linker A are diminished and the couplings between local fluctuations of residues within SH2<sub>N</sub> are enhanced upon phosphorylation.

#### 4. CONCLUSION

Results here demonstrate that effective analysis of the motion of modular, multidomain proteins includes the separation of domain motions from the total atomic displacements and a rigid-body rotation and translation of individual domains in addition to the typical overall alignment of the whole molecule extracts relative domain dynamics from local fluctuations internal to each domain. The approach enables characterization of the conformational states of multidomain proteins following a description of domain motions and local fluctuation magnitudes to relate structure and function. Functional changes in dynamics of multidomain proteins due to factors such as effector binding or phosphorylation can be effectively assessed from MD simulations with this two alignment approach. In particular, accurate estimation of LF will allow identification of possible allosteric pathways as traced from correlated fluctuations of residues<sup>4,8</sup> in multidomain proteins. We illustrated the approach here by application to the Syk tSH2 to examine the change in dynamics upon phosphorylation of Tyr-131. This chemical modification regulates the association of Syk with membrane immunoreceptors. Differences in domain-domain motion and  $C_{\alpha}$  covariance were detected between the unphosphorylated and phosphorylated forms of the Syk tSH2. Efforts are underway with more extensive sampling to understand how concerted motions internal to linker A influence, or not, the coupling of the two SH2 domains of Syk tyrosine kinase and the effects of Tyr131 phosphorylation.

## ■ ASSOCIATED CONTENT

### 📄 Supporting Information

The Supporting Information is available free of charge on the ACS Publications website at DOI: [10.1021/acs.jctc.5b00796](https://doi.org/10.1021/acs.jctc.5b00796).

One PDB formatted model trajectory with LF and DF (PDB)

One PDB formatted model trajectory with overall motion and LF and DF (PDB)

CHARMM input scripts for separation of LF and DF (PDF)

Discussions on the underdeterminacy of separation of internal motions and rigid body motion in a flexible body, separation of LF and DF when the domains are not defined properly, details of generating a model trajectory and estimation of error in separation of LF and DF, and estimation of error in interdomain correlation (PDF)

## ■ AUTHOR INFORMATION

### Corresponding Author

\*E-mail: [amitava.roy@nih.gov](mailto:amitava.roy@nih.gov).

### Notes

The authors declare no competing financial interest.

## ■ ACKNOWLEDGMENTS

We thank the Rosen Center for Advanced Computing at Purdue University for computational resources. We thank the Research Technologies Branch of National Institute of Allergy and Infectious Diseases, particularly Ryan Kissinger, for technical help with the graphics. This work was supported by National Institutes of Health Grant R01 GM039478.

## ■ REFERENCES

- (1) Zhang, Y.; Oh, H.; Burton, R. A.; Burgner, J. W.; Geahlen, R. L.; Post, C. B. *Proc. Natl. Acad. Sci. U. S. A.* **2008**, *105*, 11760–11765.
- (2) Xiao, Y.; Lee, T.; Latham, M. P.; Warner, L. R.; Tanimoto, A.; Pardi, A.; Ahn, N. G. *Proc. Natl. Acad. Sci. U. S. A.* **2014**, *111*, 2506–2511.
- (3) Esteban-Martín, S.; Fenwick, R. B.; Áden, J.; Cossins, B.; Bertoncini, C. W.; Guallar, V.; Wolf-Watz, M.; Salvatella, X. *PLoS Comput. Biol.* **2014**, *10*, e1003721.
- (4) Rivalta, I.; Sultan, M. M.; Lee, N.-S.; Manley, G.; Loria, P. J.; Batista, V. *Proc. Natl. Acad. Sci. U. S. A.* **2012**, *109*, E1428–E1436.
- (5) Li, P.; Martins, I. R.; Amarasinghe, G. K.; Rosen, M. K. *Nat. Struct. Mol. Biol.* **2008**, *15*, 613–618.
- (6) Kay, L. E.; Muhandiram, D.; Wolf, G.; Shoelson, S. E.; Forman-Kay, J. D. *Nat. Struct. Mol. Biol.* **1998**, *5*, 156–163.
- (7) Popovych, N.; Sun, S.; Ebricht, R. H.; Kalodimos, C. G. *Nat. Struct. Mol. Biol.* **2006**, *13*, 831–838.
- (8) Roy, A.; Post, C. B. *Proc. Natl. Acad. Sci. U. S. A.* **2012**, *109*, 5271–5276.
- (9) Sethi, A.; Eargle, J.; Black, A. A.; Luthey-Schulten, Z. *Proc. Natl. Acad. Sci. U. S. A.* **2009**, *106*, 6620–6625.
- (10) Ichiye, T.; Karplus, M. *Proteins: Struct., Funct., Genet.* **1991**, *11*, 205–217.
- (11) Hünenberger, P.; Mark, A.; Van Gunsteren, W. J. *Mol. Biol.* **1995**, *252*, 492–503.
- (12) Karplus, M.; Ichiye, T. *J. Mol. Biol.* **1996**, *263*, 120–122.
- (13) Zhou, Y.; Cook, M.; Karplus, M. *Biophys. J.* **2000**, *79*, 2902–2908.
- (14) Kabsch, W. *Acta Crystallogr., Sect. A: Cryst. Phys., Diffr., Theor. Gen. Crystallogr.* **1976**, *32*, 922–923.
- (15) Székely, G. J.; Rizzo, M. L.; Bakirov, N. K. *Ann. Stat.* **2007**, *35*, 2769–2794.

(16) Lange, O. F.; Grubmüller, H. *Proteins: Struct., Funct., Genet.* **2006**, *62*, 1053–1061.

(17) Roy, A.; Post, C. B. *J. Chem. Theory Comput.* **2012**, *8*, 3009–3014.

(18) Simon, N.; Tibshirani, R. *arXiv preprint arXiv:1401.7645* 2014.

(19) Young, M. A.; Gonfloni, S.; Superti-Furga, G.; Roux, B.; Kuriyan, J. *Cell* **2001**, *105*, 115–126.

(20) Littlejohn, R.; Reinsch, M. *Rev. Mod. Phys.* **1997**, *69*, 213–276.

(21) Meirovitch, E.; Shapiro, Y. E.; Liang, Z.; Freed, J. H. *J. Phys. Chem. B* **2003**, *107*, 9898–9904.

(22) Lahiri, S. *Statistics & Probability Letters* **1993**, *18*, 405–413.